

Research Article

A Turn-On Fluorescent Probe for Sensitive Detection of Cysteine in a Fully Aqueous Environment and in Living Cells

Xiaohua Ma,^{1,2} Guoguang Wu ,¹ Yuehua Zhao,³ Zibo Yuan,³ Yu Zhang,³ Ning Xia ,³ Mengnan Yang,³ and Lin Liu ³

¹School of Chemical Engineering and Technology, China University of Mining and Technology, Xuzhou, Jiangsu 221116, China

²Henan Key Laboratory of Biomolecular Recognition and Sensing, College of Chemistry and Chemical Engineering, Shangqiu Normal University, Shangqiu, Henan 476000, China

³Key Laboratory of New Optoelectronic Functional Materials (Henan Province), College of Chemistry and Chemical Engineering, Anyang Normal University, Anyang, Henan 455000, China

Correspondence should be addressed to Guoguang Wu; tb12040004@cumt.edu.cn, Ning Xia; xianing82414@163.com, and Lin Liu; liulin@aynu.edu.cn

Received 30 July 2018; Revised 6 October 2018; Accepted 15 October 2018; Published 13 December 2018

Academic Editor: Chih-Ching Huang

Copyright © 2018 Xiaohua Ma et al. This is an open access article distributed under the Creative Commons Attribution License, which permits unrestricted use, distribution, and reproduction in any medium, provided the original work is properly cited.

We reported here a turn-on fluorescent probe (**1**) for the detection of cysteine (Cys) by incorporating the recognition unit of 2,4-dinitrobenzenesulfonyl ester (DNBS) to a coumarin derivative. The structure of the obtained probe was confirmed by NMR and HRMS techniques. The probe shows a remarkable fluorescence off-on response (~52-fold) by the reaction with Cys in 100% aqueous buffer. The sensing mechanism was verified by the HPLC test. Probe **1** also displays high selectivity towards Cys. The detection limit was calculated to be 23 nM. Moreover, cellular experiments demonstrated that the probe is highly biocompatible and can be used for monitoring intracellular Cys.

1. Introduction

Cysteine (Cys), a kind of critical biothiols, plays many crucial physiological roles, such as maintaining biological redox homeostasis, participation in enzymatic reactions, and sequestering inimical metal ions [1–4]. The abnormal levels of Cys are associated with many syndromes and diseases, including growth retarding, muscle loss, skin lesions, liver damage, severe neurotoxicity, and cardiovascular diseases [5–7]. Therefore, it is highly desired to develop effective Cys assays for application in biological systems, which would be very helpful to further elucidate its biological functions and reveal its relevance to certain diseases.

Analytical methods for the detection of Cys include capillary electrophoresis (CE) [8–10], highperformance liquid chromatography (HPLC) [11–13], electrochemical methods [14], and colorimetric and fluorescent assays [3, 15–18]. Among them, the fluorescence assay based on

optical probes has gained tremendous attentions due to its inherent advantages of high sensitivity and selectivity, simplicity of implementation, high spatiotemporal resolution, and good compatibility for biosamples [19–26]. Up to now, some fluorescent probes have been synthesized for the detection of Cys by exploiting mechanisms of Michael addition, cleavage of the selenium-nitrogen bond and of disulfides, cyclization with aldehydes, cleavage of sulfonamide and sulfonate esters, and metal complex replacement of ligands [27–40]. However, many of these developed probes have drawbacks of low sensitivity, complicated synthetic process, and/or the use of high-content organic solvent. Thus, developing facile and reliable fluorescent Cys probes is still highly desired. Herein, we report a highly sensitive fluorogenic Cys probe (**1**) by installing the recognition moiety of 2,4-dinitrobenzenesulfonyl ester (DNBS) onto a coumarin fluorophore. Coumarin and its derivatives are popular fluorescent reporters due to their

high photostability, excellent biocompatibility, and high quantum yield [41–43]. Upon the target-mediated cleavage of 2,4-dinitrobenzenesulfonyl ester and release of the coumarin fluorophore, probe **1** exhibits efficient turn-on fluorescent response towards Cys. Moreover, the proposed probe **1** displays good water solubility, high sensitivity and selectivity, and low cytotoxicity and can be used for imaging intracellular Cys.

2. Experimental Section

2.1. General Procedure for Analysis. All spectral measurements were performed in the aqueous phosphate buffer (pH 7.4, 10 mM). Stock solution of probe **1** (0.1 mM) was prepared in the same phosphate buffer solution. The following solutions (10.0 mM) were prepared in deionized water: amino acids (Cys, Hcy, GSH, Gly, Ser, Val, Leu, Tyr, His, Trp, Arg, Glu, Pro, Asp, Thr, Asn, and Phe), ascorbic acid (AA), and glutathione (GSH). Test solutions were prepared by placing 300.0 μ L of stock solution **1** (0.1 mM), an appropriate aliquot of each analyte stock solution into a 5.0 mL centrifugal tube, and diluting the solution to 3.0 mL with the phosphate buffer (pH 7.4, 10 mM). The solution was mixed for a given time at the room temperature. Then, the fluorescence and UV absorption spectra were recorded. For fluorescence assays, the excitation and emission slit width are both 5 nm.

2.2. Synthesis of Probe 1. Synthesis procedures for probe **1** were displayed in Scheme 1. Compound **3** was obtained according to literature methods [44, 45].

Compound **2**, compound **3** (12.8 g, 50 mmol), 2,3,6,7-tetrahydro-8-hydroxy-1H, and 5H-benz[*i*, *j*]quinolizine-9-carboxaldehyde (8.26 g, 50 mmol) were added to toluene (0.1 L), and the mixture was refluxed for 10 h. Then, the formed solid product was filtered and washed with hexanes. The obtained precipitation was further dried under vacuum giving a white solid (8.7 g, 76%). ^1H NMR (400 MHz, DMSO) δ : 11.78 (s, 1H), 7.19 (d, $J = 31.3$ Hz, 1H), 5.22 (s, 1H), 3.23 (s, 4H), 2.70 (s, 4H), and 1.87 (s, 4H) (Figure S1). ^{13}C NMR (100 MHz, DMSO): δ 167.06 (s), 163.29 (s), 151.46 (s), 146.45 (s), 120.35 (s), 117.78 (s), 105.80 (s), 103.53 (s), 86.25 (s), 49.67 (s), 49.14 (s), 27.42 (s), 21.46 (s), and 20.58 (d, $J = 2.3$ Hz) (Figure S2). HRMS: m/z , calcd. $[\text{M} + \text{H}]^+$ 258.1130; found 258.1126 (Figure S3).

Probe **1** was prepared by reacting compound **2** with 2,4-dinitrobenzenesulfonyl chloride. In brief, compound **2** (2.57 g, 10 mmol), 2,4-dinitrobenzenesulfonyl chloride (2.67 g, 10 mmol), and triethylamine (1.21 g, 12 mmol) were added in anhydrous CH_2Cl_2 (0.1 L) at 0°C . After stirring for 1 h, the mixture was gradually warmed to the room temperature and reacted for another 2 h. Then, the reaction mixture was evaporated to dryness and purified by column chromatography (silica, DCM-EtOAc as eluent, 2: 1, v/v) yielded **1** as a yellow solid (12.82 g, 58%). ^1H NMR (400 Hz, CDCl_3): δ 8.71 (s, 1H), 8.60 (d, $J = 8.1$ Hz, 1H), 8.41 (d, $J = 8.3$ Hz, 1H), 7.16 (s, 1H), 5.87 (s, 1H), 3.30 (s, 4H), 2.79 (d, $J = 35.0$ Hz,

4H), and 1.96 (s, 4H) (Figure S4). ^{13}C NMR (101 MHz, CDCl_3) δ 161.98 (s), 158.41 (s), 151.30 (s), 151.19 (s), 148.87 (s), 134.00 (s), 133.36 (s), 126.96 (s), 120.79 (s), 120.06 (s), 119.25 (s), 96.54 (s), 77.34 (s), 77.23 (s), 77.03 (s), 76.71 (s), 50.11 (s), 49.67 (s), 27.54 (s), 21.06 (s), 20.31 (s), and 20.13 (s) (Figure S5). HRMS: m/z , calcd. $[\text{M} + \text{H}]^+$ 488.0764; found 488.0759 (Figure S6).

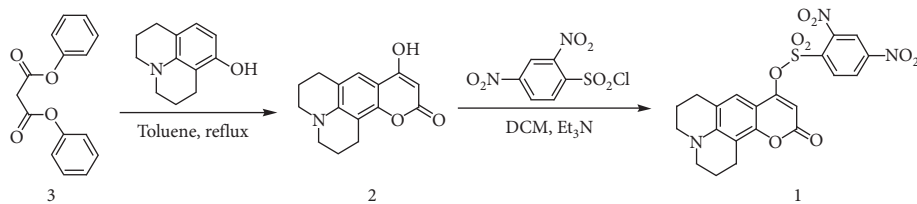
3. Results and Discussion

3.1. Design and Synthesis. The probe **1** was devised by exploiting **2** as the fluorophore and DNBS as the reaction moiety. The coumarin derivative (compound **2**) was selected here because of its high emission efficiency, facile preparation procedure, excellent water solubility, and biocompatibility. DNBS group has been exploited as a good reaction moiety for fluorescent biothiols probes. Scheme 1 illustrates the synthesis procedures for probe **1**. Compound **2** was prepared via refluxing malonate ester with 2,3,6,7-tetrahydro-8-hydroxy-1H and 5H-benz[*i*, *j*]quinolizine in toluene. Furthermore, coupling **2** with 2,4-dinitrobenzenesulfonyl chloride in CH_2Cl_2 afforded **1**. The structures of compound **2** and probe **1** were confirmed by NMR and HRMS (Supporting Information).

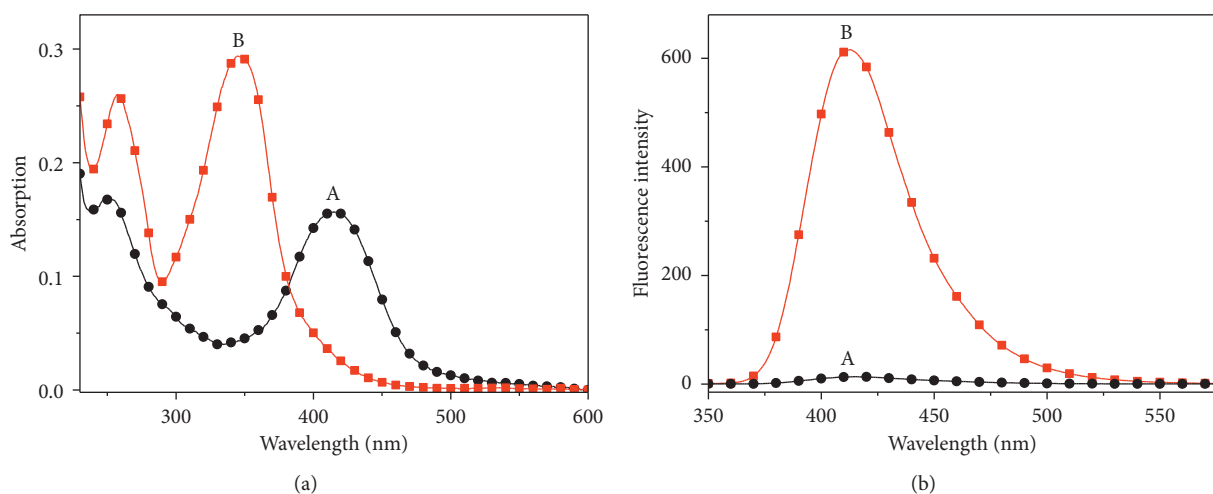
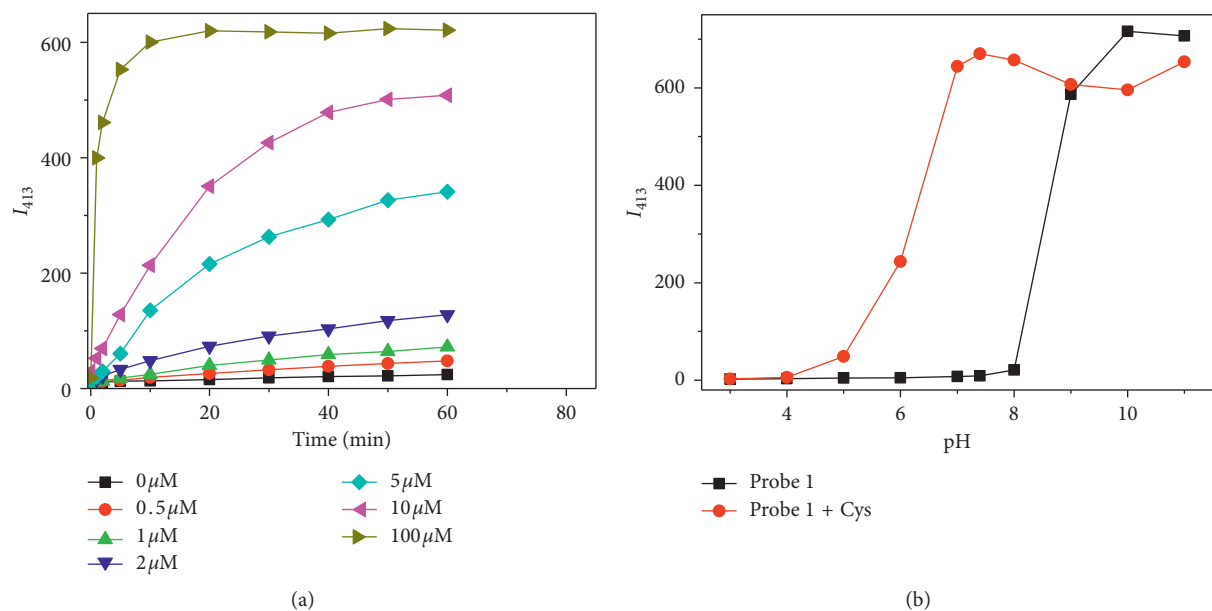
3.2. Spectral Characteristics of Probe 1 and Its Optical Responses towards Cys. The spectroscopic characteristics of probe **1** were inspected with or without Cys (10.0 equiv) (Figure 1). **1** alone displayed an absorption band at about 415 nm ($\epsilon = 1.57 \times 10^4 \text{ M}^{-1} \cdot \text{cm}^{-1}$) and nonemissivity (curve a). With the addition of Cys (10.0 equiv), the absorbance at 415 nm decreased significantly, and a new absorption band centered at 347 nm ($\epsilon = 2.93 \times 10^4 \text{ M}^{-1} \cdot \text{cm}^{-1}$) appeared (curve b). Meanwhile, the emission of the probe solution increased remarkably ($\lambda_{\text{em}} = 413$ nm). These obvious spectral responses imply that probe **1** is capable of monitoring Cys.

To study the response time of probe **1** for Cys, time-dependent fluorescence response of probe **1** towards Cys with different concentrations was investigated (Figure 2(a)). The peak emission intensity of probe **1** did not obviously change in the absence of Cys during the time course of testing, indicating the high stability of the probe in the aqueous buffer solution under the neutral condition. And the emission intensity was observed to increase in the presence of Cys in a concentration-dependent fashion. Higher concentration of Cys (ca. 10.0 equiv) afforded a quicker and more dramatic fluorescent response. The pseudofirst-order rate of the reaction is found to be $1.4 \times 10^{-2} \cdot \text{s}^{-1}$ (Figure S7). And 1 h was set as the optimized reaction time as the fluorescence intensity reached a plateau within 1 h at each inspected concentration of Cys.

The effect of pH on the response of **1** toward Cys was studied. Without Cys, the fluorescence intensity of the probe remained unchanged with $\text{pH} \leq 8$ and increased significantly with the pH value over 8, indicating that probe **1** is stable under the neutral condition and prone to hydrolysis under



SCHEME 1: Synthetic route for probe 1.

FIGURE 1: (a) Absorption and (b) emission spectra of probe 1 ($10 \mu\text{M}$) in the absence (A) and presence (B) of Cys ($100 \mu\text{M}$) in a solution of the phosphate buffer (pH 7.4, 10 mM). $\lambda_{\text{ex}} = 347 \text{ nm}$.FIGURE 2: (a) Time-dependent fluorescence intensity changes of probe 1 ($10 \mu\text{M}$) at 413 nm in the presence of various concentrations of Cys (0, 0.5, 1, 2, 5, 10, and $100 \mu\text{M}$); (b) effect of pH on the fluorescence response of probe 1 ($10 \mu\text{M}$) towards Cys ($100 \mu\text{M}$). $\lambda_{\text{ex}} = 347 \text{ nm}$.

the alkaline condition (Figure 2(b)). With addition of Cys, the fluorescence was gradually increased in the region of pH 4.0–7.0 and reached the maximum at pH 7.4. These results demonstrated that 1 responds well to Cys at round physiological pH.

3.3. Sensitivity and Selectivity. The quantitative response ability of probe 1 towards Cys was inspected via fluorescence titration. The fluorescence intensity gradually increases with increment of Cys contents and reaches a plateau with the Cys concentration up to $30 \mu\text{M}$ (Figure 3). And there is a good

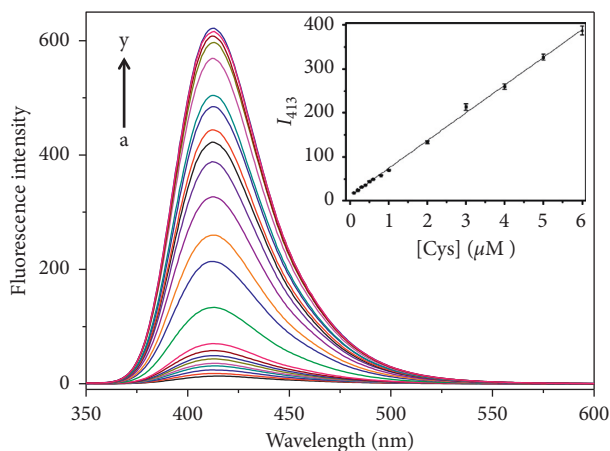


FIGURE 3: Fluorescence spectra of probe **1** ($10\ \mu\text{M}$) in the presence of Cys with various concentrations: 0, 0.1, 0.2, 0.3, 0.4, 0.5, 0.6, 0.8, 1.0, 2.0, 3.0, 4.0, 5.0, 6.0, 7.0, 8.0, 9.0, 10.0, 20.0, 30.0, 40.0, 50.0, and $100.0\ \mu\text{M}$ (from *a* to *y*). Inset shows the standard curve. $\lambda_{\text{ex}} = 347\ \text{nm}$.

linear correlation between emission intensity at 413 nm and the Cys concentration in the range of $0.1\text{--}6\ \mu\text{M}$. Linear equation can be expressed as $I = 10.81 + 63.16 \times [\text{Cys}]/\mu\text{M}$ ($R^2 = 0.998$). The detection limit was estimated to be $23\ \text{nM}$ (3σ). The analytical performances of probe **1** were also compared with other reported fluorescent Cys probes using 2,4-dinitrobenzenesulfonyl ester (DNBS) as the recognition moiety [46–55] (Table S1).

To evaluate the specificity of the assay, the spectral response of probe **1** towards various biologically relevant analytes including twenty natural protein amino acids, AA, Hcy, and GSH was recorded. Cys generated a significant enhancement of fluorescence intensity. Another biothiol, Hcy, also created an obvious fluorescent emission for the probe solution, indicating that probe **1** can response to both Cys and Hcy but showing a higher reactivity for Cys. Other analytes, including GSH, did not show any significant changes (Figure 4(a)). The higher reactivity of the probe toward Cys over GSH may be ascribed to the bulkiness of GSH and the significant steric hindrance around its thiol group. The spectral response of probe **1** for various metal ions (Al^{3+} , Ca^{2+} , Cd^{2+} , Co^{2+} , Cu^{2+} , Fe^{2+} , Fe^{3+} , K^+ , Mg^{2+} , Mn^{2+} , Na^+ , Ni^{2+} , Pb^{2+} , and Zn^{2+}) was also inspected (Figure S8), indicating that probe **1** is nonresponsive for these metal ions. Furthermore, competition experiments also indicated that the coexistence of other interfering species did not influence the reactivity of probe **1** for Cys (Figure 4(b)).

3.4. Sensing Mechanism. The presented fluorescent Cys probe (**1**) was obtained by incorporating the DNBS functional group (a well-known recognition moiety for the biothiols) onto the coumarin-based fluorophore. Probe **1** is nonfluorescent due to the quenching effect of DNBS unit via the electron-transfer process. The introduced Cys can first react with DNBS of the probe via the nucleophilic aromatic substitution and form a unstable negative-charged intermediate, which further involved the intramolecular rearrangement to yield the sulfur dioxide, 2,4-dinitrophenyl cysteine, and compound **2** (a highly-emissive

fluorophore) (Scheme 2). HPLC analysis was performed to verify this proposed sensing mechanism. **1** alone exhibited a single chromatographic peak at 2.00 min (curve *a* in Figure 5). After incubation probe **1** ($10\ \mu\text{M}$) with Cys ($5\ \mu\text{M}$), a new peak at 0.56 min appeared, which can be ascribed to compound **2** (curves *b* and *d* in Figure 5). Incubating probe **1** ($10\ \mu\text{M}$) with high concentration of Cys ($100\ \mu\text{M}$) resulted in the disappearance of the peak at 2.00 min and led to a chromatographic profile identical to that of compound **2**, which indicated that probe **1** can be completely converted to compound **2** upon the Cys-induced thiolysis process.

3.5. Cellular Imaging. The good water solubility and high selectivity inspired us to use **1** for the bioimaging application. Firstly, cellular cytotoxicity of probe **1** was inspected (Figure S9). The high survival rates of all these three kinds of cells with different concentrations of probe **1** indicated that the probe was highly biocompatible. Then, cellular imaging experiments were conducted. HeLa cells incubated with probe **1** alone displayed no intracellular fluorescence (Figure 6(b)). However, cells incubated with **1** and consequently with Cys ($100\ \mu\text{M}$) exhibited strong blue fluorescent emission (Figure 6(e)). These imaging results indicated that probe **1** is living cell membrane permeable and can be used to monitor intracellular Cys.

4. Conclusions

In conclusion, we developed a turn-on fluorescent probe for Cys based on a coumarin-derived fluorophore. The sensing mechanism involved the Cys-induced cleavage of the DNBS group and the follow-up release of the coumarin fluorophore, which was confirmed by HPLC and spectral results. Probe **1** displayed high selectivity for Cys and a low detection limit of $23\ \text{nM}$. The proposed probe also features excellent water solubility and biocompatibility and has been successfully utilized for imaging Cys in living cells.

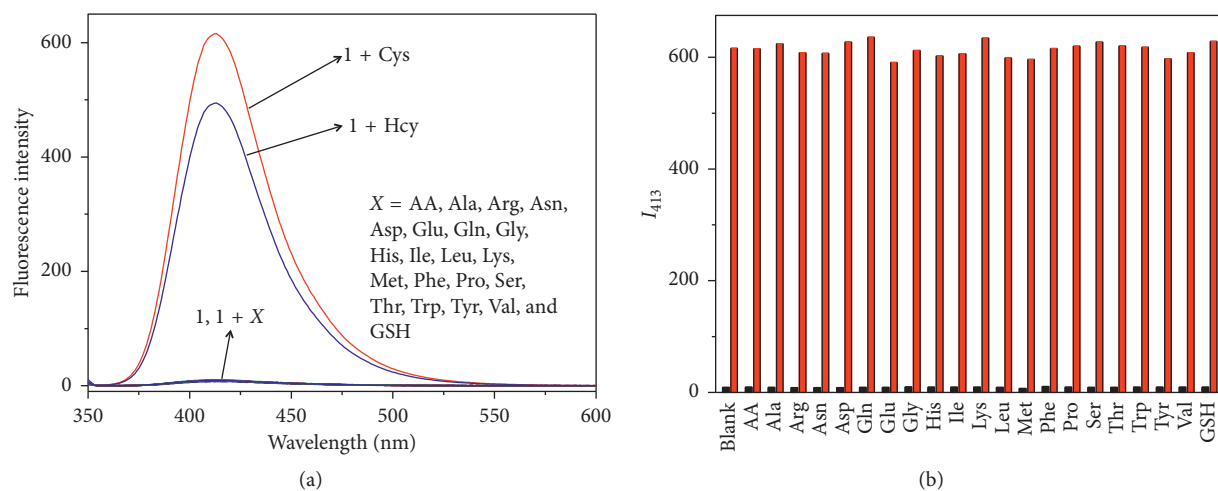
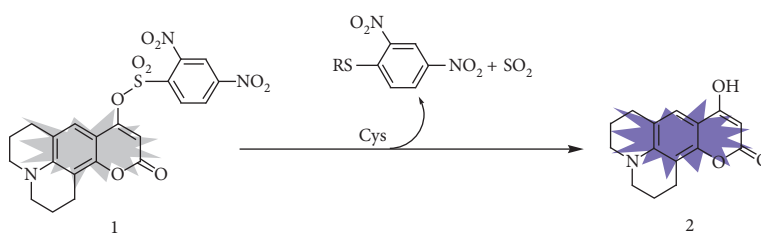


FIGURE 4: (a) Fluorescence spectra of probe 1 (10 μM) towards different amino acids, AA and GSH (100 μM). (b) Fluorescence intensities of probe 1 (10 μM) at 413 nm upon the addition of different interfering species (100 μM) (low bars), followed by addition of Cys (100 μM) (high bars). $\lambda_{\text{ex}} = 347$ nm.



SCHEME 2: Sensing mechanism of probe 1 for Cys.

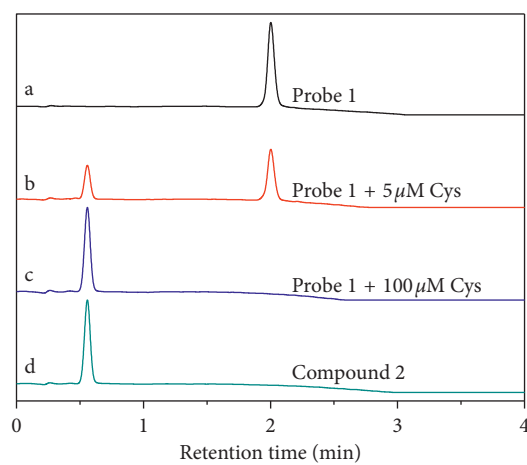


FIGURE 5: Reversed-phase HPLC chromatograms of (a) probe 1 (10 μM), (b) probe 1 (10 μM) and Cys (5 μM), (c) probe 1 (10 μM) and Cys (100 μM), and (d) compound 2.

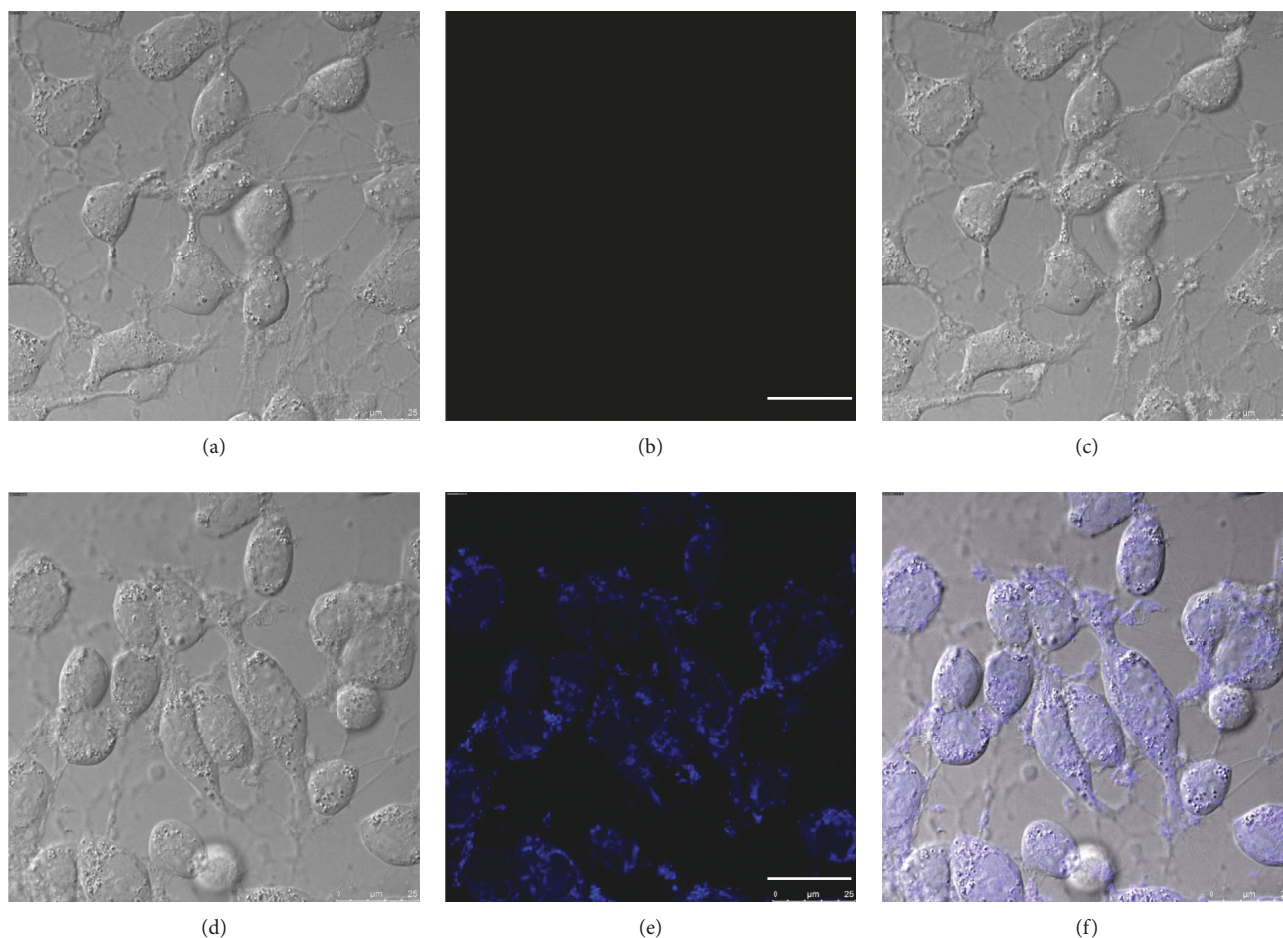


FIGURE 6: Confocal fluorescence images of living HeLa cells. Bright-field image (a) and fluorescence image (b) of cells incubated with probe **1** ($10\ \mu\text{M}$) for 1 h; (c) overlay of the images of (a) and (b); bright-field image (d) and fluorescence image (e) of cells incubated with probe **1** ($10\ \mu\text{M}$) for 1 h and subsequent treatment with Cys ($100\ \mu\text{M}$) for another 1 h; (f) overlay of the images of (d) and (e). $\lambda_{\text{ex}} = 405\ \text{nm}$; scale bar = $25\ \mu\text{m}$.

Data Availability

The data used to support the findings of this study are available from the corresponding author upon request.

Conflicts of Interest

The authors declare that there are no conflicts of interest regarding the publication of this article.

Acknowledgments

We are grateful to the Program for Science and Technology Innovation Talents at the University of Henan Province (18HASTIT005), the Fund Project for Young Scholar sponsored by Henan Province (2016GGJS-122), and the Program for Innovative Research Team of Science and Technology in the University of Henan Province (18IRT-STHN004) for support.

Supplementary Materials

Supplementary Description Part 1: experimental materials, instrumentations, and experimental procedures for the HPLC test and cell viability assay/imaging. Part 2: characterization of compound **2** and probe **1**. Figure S1: ^1H NMR chemical shifts of compound **2**. Figure S2: ^{13}C NMR chemical shifts of compound **2**. Figure S3: high-resolution mass spectrum (HRMS) of compound **2**. Figure S4: ^1H NMR chemical shifts of probe **1**. Figure S5: ^{13}C NMR chemical shifts of probe **1**. Figure S6: high-resolution mass spectrum (HRMS) of probe **1**. Part 3: kinetic study of **1** to Cys. Figure S7: the kinetic study of the response of probe **1** to Cys (10 equiv) under pseudofirst-order conditions based on the time course of the emission intensity at 413 nm. Part 4: comparison of DNBS-based fluorescent probes for Cys. Table S1: comparison of DNBS-based fluorescent probes for Cys. Part 5: spectral responses of probe **1** for various metal ions. Figure S8: fluorescence intensities of probe **1** ($10\ \mu\text{M}$) at 413 nm upon the addition of Cys ($100\ \mu\text{M}$) and different metal ions ($100\ \mu\text{M}$); $\lambda_{\text{ex}} = 347\ \text{nm}$. Part

6: cell cytotoxicity of probe **1**. Figure S9: cell cytotoxicity of probe **1** against HeLa, A549, and MDA-MB-231 cells upon 24 h of incubation. (*Supplementary Materials*)

References

- [1] K. G. Reddie and K. S. Carroll, "Expanding the functional diversity of proteins through cysteine oxidation," *Current Opinion in Chemical Biology*, vol. 12, no. 6, pp. 746–754, 2008.
- [2] T. Dudev and C. Lim, "Metal binding affinity and selectivity in metalloproteins: insights from computational studies," *Annual Review of Biophysics*, vol. 37, no. 1, pp. 97–116, 2008.
- [3] X. Chen, Y. Zhou, X. Peng, and J. Yoon, "Fluorescent and colorimetric probes for detection of thiols," *Chemical Society Reviews*, vol. 39, no. 6, pp. 2120–2135, 2010.
- [4] C. E. Paulsen and K. S. Carroll, "Cysteine-mediated redox signaling: chemistry, biology, and tools for discovery," *Chemical Reviews*, vol. 113, no. 7, pp. 4633–4679, 2013.
- [5] W. Dröge, H. P. Eck, and S. Mihm, "HIV-induced cysteine deficiency and T-cell dysfunction—a rationale for treatment with N-acetylcysteine," *Immunology Today*, vol. 13, no. 6, pp. 211–214, 1992.
- [6] M. W. Lieberman, A. L. Wiseman, Z. Z. Shi et al., "Growth retardation and cysteine deficiency in gamma-glutamyl transpeptidase-deficient mice," *Proceedings of the National Academy of Sciences*, vol. 93, no. 15, pp. 7923–7926, 1996.
- [7] J. A. McMahon, T. J. Green, C. M. Skeaff, R. G. Knight, J. I. Mann, and S. M. Williams, "A controlled trial of homocysteine lowering and cognitive performance," *New England Journal of Medicine*, vol. 354, no. 26, pp. 2764–2772, 2006.
- [8] A. V. Ivanov, E. D. Virus, B. P. Luzyanin, and A. A. Kubatiev, "Capillary electrophoresis coupled with 1,1'-thiocarbonyldiimidazole derivatization for the rapid detection of total homocysteine and cysteine in human plasma," *Journal of Chromatography B*, vol. 1004, pp. 30–36, 2015.
- [9] J. Lacna, F. Foret, and P. Kuban, "Capillary electrophoresis in the analysis of biologically important thiols," *Electrophoresis*, vol. 38, no. 1, pp. 203–222, 2017.
- [10] K. Y. Liu, H. Wang, J. L. Bai, and L. Wang, "Home-made capillary array electrophoresis for high-throughput amino acid analysis," *Analytica Chimica Acta*, vol. 622, no. 1–2, pp. 169–174, 2008.
- [11] L. Y. Zhang, F. Q. Tu, X. F. Guo, H. Wang, P. Wang, and H. S. Zhang, "A new BODIPY-based long-wavelength fluorescent probe for chromatographic analysis of low-molecular-weight thiols," *Analytical and Bioanalytical Chemistry*, vol. 406, no. 26, pp. 6723–6733, 2014.
- [12] L. J. Zhang, B. Q. Lu, C. Lu, and J. M. Lin, "Determination of cysteine, homocysteine, cystine, and homocystine in biological fluids by HPLC using fluorosurfactant-capped gold nanoparticles as postcolumn colorimetric reagents," *Journal of Separation Science*, vol. 37, no. 1–2, pp. 30–36, 2014.
- [13] D. Tsikas, J. Sandmann, M. Ikić, J. Fauler, D. O. Stichtenoth, and J. C. Frolich, "Analysis of cysteine and N-acetylcysteine in human plasma by high-performance liquid chromatography at the basal state and after oral administration of N-acetylcysteine," *Journal of Chromatography B*, vol. 708, no. 1–2, pp. 55–60, 1998.
- [14] P. T. Lee, D. Lowinsohn, and R. G. Compton, "Simultaneous detection of homocysteine and cysteine in the presence of ascorbic acid and glutathione using a nanocarbon modified electrode," *Electroanalysis*, vol. 26, no. 7, pp. 1488–1496, 2014.
- [15] Y. Q. Hao, D. D. Xiong, L. Q. Wang, W. S. Chen, B. B. Zhou, and Y. N. Liu, "A reversible competition colorimetric assay for the detection of biothiols based on ruthenium-containing complex," *Talanta*, vol. 115, pp. 253–257, 2013.
- [16] D. Y. Lee, G. M. Kim, J. Yin, and J. Yoon, "An aryl-thioether substituted nitrobenzothiadiazole probe for the selective detection of cysteine and homocysteine," *Chemical Communications*, vol. 51, no. 30, pp. 6518–6520, 2015.
- [17] L. Cui, Y. Baek, S. Lee, N. Kwon, and J. Yoon, "An AIE and ESIPT based kinetically resolved fluorescent probe for biothiols," *Journal of Materials Chemistry C*, vol. 4, no. 14, pp. 2909–2914, 2016.
- [18] B. Babur, N. Seferoglu, M. Ocal, G. Sonugur, H. Akbulut, and Z. Seferoglu, "A novel fluorescence turn-on coumarin-pyrazolone based monomethine probe for biothiol detection," *Tetrahedron*, vol. 72, no. 30, pp. 4498–4502, 2016.
- [19] N. Xia, B. Zhou, N. Huang, M. Jiang, J. Zhang, and L. Liu, "Visual and fluorescent assays for selective detection of beta-amyloid oligomers based on the inner filter effect of gold nanoparticles on the fluorescence of CdTe quantum dots," *Biosensors and Bioelectronics*, vol. 85, pp. 625–632, 2016.
- [20] Y. Q. Hao, Y. T. Zhang, K. H. Ruan et al., "A naphthalimide-based chemodosimetric probe for ratiometric detection of hydrazine," *Sensors and Actuators B-Chemical*, vol. 244, pp. 417–424, 2017.
- [21] W. Q. Chen, X. X. Yue, H. Zhang et al., "Simultaneous detection of glutathione and hydrogen polysulfides from different emission channels," *Analytical Chemistry*, vol. 89, no. 23, pp. 12984–12991, 2017.
- [22] X. H. Li, X. H. Gao, W. Shi, and H. M. Ma, "Design strategies for water-soluble small molecular chromogenic and fluorogenic probes," *Chemical Reviews*, vol. 114, no. 1, pp. 590–659, 2014.
- [23] L. Yuan, W. Y. Lin, K. B. Zheng, L. W. He, and W. M. Huang, "Far-red to near infrared analyte-responsive fluorescent probes based on organic fluorophore platforms for fluorescence imaging," *Chemical Society Reviews*, vol. 42, no. 2, pp. 622–661, 2013.
- [24] M. La, Y. Q. Hao, Z. Y. Wang, G. C. Han, and L. B. Qu, "Selective and sensitive detection of cyanide based on the displacement strategy using a water-soluble fluorescent probe," *Journal of Analytical Methods in Chemistry*, vol. 2016, Article ID 1462013, 6 pages, 2016.
- [25] Y. Jung, J. Jung, Y. Huh, and D. Kim, "Benzo-g-coumarin-based fluorescent probes for bioimaging applications," *Journal of Analytical Methods in Chemistry*, vol. 2018, Article ID 5249765, 11 pages, 2018.
- [26] L. Liu, Y. Chang, J. Yu, M. S. Jiang, and N. Xia, "Two-in-one polydopamine nanospheres for fluorescent determination of beta-amyloid oligomers and inhibition of beta-amyloid aggregation," *Sensors and Actuators B-Chemical*, vol. 251, pp. 359–365, 2017.
- [27] H. S. Jung, X. Q. Chen, J. S. Kim, and J. Yoon, "Recent progress in luminescent and colorimetric chemosensors for detection of thiols," *Chemical Society Reviews*, vol. 42, no. 14, pp. 6019–6031, 2013.
- [28] L. Y. Niu, Y. Z. Chen, H. R. Zheng, L. Z. Wu, C. H. Tung, and Q. Z. Yang, "Design strategies of fluorescent probes for selective detection among biothiols," *Chemical Society Reviews*, vol. 44, no. 17, pp. 6143–6160, 2015.

- [29] H. Chen, Y. H. Tang, and W. Y. Lin, "Recent progress in the fluorescent probes for the specific imaging of small molecular weight thiols in living cells," *Trac-Trends in Analytical Chemistry*, vol. 76, pp. 166–181, 2016.
- [30] C. Yin, F. Huo, J. Zhang et al., "Thiol-addition reactions and their applications in thiol recognition," *Chemical Society Reviews*, vol. 42, no. 14, pp. 6032–6059, 2013.
- [31] Y. Geng, H. Tian, L. Yang, X. Liu, and X. Song, "An aqueous methylated chromenoquinoline-based fluorescent probe for instantaneous sensing of thiophenol with a red emission and a large Stokes shift," *Sensors and Actuators B: Chemical*, vol. 273, pp. 1670–1675, 2018.
- [32] X. Ren, H. Tian, L. Yang et al., "Fluorescent probe for simultaneous discrimination of Cys/Hcy and GSH in pure aqueous media with a fast response under a single-wavelength excitation," *Sensors and Actuators B: Chemical*, vol. 273, pp. 1170–1178, 2018.
- [33] S. Zhou, Y. Rong, H. Wang, X. Liu, L. Wei, and X. Song, "A naphthalimide-indole fused chromophore-based fluorescent probe for instantaneous detection of thiophenol with a red emission and a large Stokes shift," *Sensors and Actuators B: Chemical*, vol. 276, pp. 136–141, 2018.
- [34] Y. Wang, L. Wang, E. Jiang et al., "A colorimetric and ratiometric dual-site fluorescent probe with 2,4-dinitrobenzenesulfonyl and aldehyde groups for imaging of aminothiols in living cells and zebrafish," *Dyes and Pigments*, vol. 156, pp. 338–347, 2018.
- [35] Y. Wang, M. Zhu, E. Jiang, R. Hua, R. Na, and Q. X. Li, "A simple and rapid turn on ESIPT fluorescent probe for colorimetric and ratiometric detection of biothiols in living cells," *Scientific Reports*, vol. 7, no. 1, p. 4377, 2017.
- [36] R. Na, M. Zhu, S. Fan et al., "A simple and effective ratiometric fluorescent probe for the selective detection of cysteine and homocysteine in aqueous media," *Molecules*, vol. 21, no. 8, p. 1023, 2016.
- [37] L. Xia, Y. Zhao, J. Huang, Y. Gu, and P. Wang, "A fluorescent turn-on probe for highly selective detection of cysteine and its bioimaging applications in living cells and tissues," *Sensors and Actuators B: Chemical*, vol. 270, pp. 312–317, 2018.
- [38] P. Wang, Q. Wang, J. Huang, N. Li, and Y. Gu, "A dual-site fluorescent probe for direct and highly selective detection of cysteine and its application in living cells," *Biosensors and Bioelectronics*, vol. 92, pp. 583–588, 2017.
- [39] Q. Wang, H. Wang, J. Huang, N. Li, Y. Gu, and P. Wang, "Novel NIR fluorescent probe with dual models for sensitively and selectively monitoring and imaging Cys in living cells and mice," *Sensors and Actuators B: Chemical*, vol. 253, pp. 400–406, 2017.
- [40] P. Wang, Y. Wang, N. Li, J. Huang, Q. Wang, and Y. Gu, "A novel DCM-NBD conjugate fluorescent probe for discrimination of Cys/Hcy from GSH and its bioimaging applications in living cells and animals," *Sensors and Actuators B: Chemical*, vol. 245, pp. 297–304, 2017.
- [41] Y. Hao, W. Chen, L. Wang et al., "A retrievable, water-soluble and biocompatible fluorescent probe for recognition of Cu(II) and sulfide based on a peptide receptor," *Talanta*, vol. 143, pp. 307–314, 2015.
- [42] D. T. Gryko, J. Piechowska, and M. Gałżowski, "Strongly emitting fluorophores based on 1-azaperylene scaffold," *Journal of Organic Chemistry*, vol. 75, no. 4, pp. 1297–1300, 2010.
- [43] R. Nazir, A. J. Stasyuk, and D. T. Gryko, "Vertically π -expanded coumarins: the synthesis and optical properties," *Journal of Organic Chemistry*, vol. 81, no. 22, pp. 11104–11114, 2016.
- [44] X. Shi, F. Huo, J. Chao, and C. Yin, "A ratiometric fluorescent probe for hydrazine based on novel cyclization mechanism and its application in living cells," *Sensors and Actuators B: Chemical*, vol. 260, pp. 609–616, 2018.
- [45] J. Liu, Y.-Q. Sun, Y. Huo et al., "Simultaneous fluorescence sensing of Cys and GSH from different emission channels," *Journal of the American Chemical Society*, vol. 136, no. 2, pp. 574–577, 2014.
- [46] H. Maeda, H. Matsuno, M. Ushida, K. Katayama, K. Saeki, and N. Itoh, "2,4-Dinitrobenzenesulfonyl fluoresceins as fluorescent alternatives to ellman's reagent in thiol-quantification enzyme assays," *Angewandte Chemie International Edition*, vol. 44, no. 19, pp. 2922–2925, 2005.
- [47] J. Bouffard, Y. Kim, T. M. Swager, R. Weissleder, and S. A. Hilderbrand, "A highly selective fluorescent probe for thiol bioimaging," *Organic Letters*, vol. 10, no. 1, pp. 37–40, 2008.
- [48] M. Wei, P. Yin, Y. Shen et al., "A new turn-on fluorescent probe for selective detection of glutathione and cysteine in living cells," *Chemical Communications*, vol. 49, no. 41, pp. 4640–4642, 2013.
- [49] Y. Liu, K. Xiang, B. Tian, and J. Zhang, "A fluorescein-based fluorescence probe for the fast detection of thiol," *Tetrahedron Letters*, vol. 57, no. 23, pp. 2478–2483, 2016.
- [50] X.-D. Jiang, J. Zhang, X. Shao, and W. Zhao, "A selective fluorescent turn-on NIR probe for cysteine," *Organic & Biomolecular Chemistry*, vol. 10, no. 10, pp. 1966–1968, 2012.
- [51] J. Shao, H. Sun, H. Guo et al., "A highly selective red-emitting FRET fluorescent molecular probe derived from BODIPY for the detection of cysteine and homocysteine: an experimental and theoretical study," *Chemical Science*, vol. 3, no. 4, pp. 1049–1061, 2012.
- [52] J. Shao, H. Guo, S. Ji, and J. Zhao, "Styryl-BODIPY based red-emitting fluorescent OFF-ON molecular probe for specific detection of cysteine," *Biosensors and Bioelectronics*, vol. 26, no. 6, pp. 3012–3017, 2011.
- [53] W. Qu, L. Yang, Y. Hang, X. Zhang, Y. Qu, and J. Hua, "Photostable red turn-on fluorescent diketopyrrolopyrrole chemodosimeters for the detection of cysteine in living cells," *Sensors and Actuators B: Chemical*, vol. 211, pp. 275–282, 2015.
- [54] C. Yin, W. Zhang, T. Liu, J. Chao, and F. Huo, "A near-infrared turn on fluorescent probe for biothiols detection and its application in living cells," *Sensors and Actuators B: Chemical*, vol. 246, pp. 988–993, 2017.
- [55] S. Chen, H. Li, and P. Hou, "Imidazo[1,5- α]pyridine-derived fluorescent turn-on probe for cellular thiols imaging with a large Stokes shift," *Tetrahedron Letters*, vol. 58, no. 27, pp. 2654–2657, 2017.



Hindawi

Submit your manuscripts at
www.hindawi.com

